

Supplemental information for:

A medium-firm drug-candidate library of cryptand-like structures on T7 phage: design and selection of a strong binder for Hsp90

Kazuto Mochizuki,^{‡a§} Lisa Matsukura,^{‡b} Yuji Ito,^c Naoyuki Miyashita^{*a,b}
and Masumi Taki^{*a}

^a *Department of Engineering Science, Bioscience and Technology Program, The Graduate School of Informatics and Engineering, The University of Electro-Communications (UEC), 1-5-1 Chofugaoka, Chofu, Tokyo 182-8585, Japan.*

Tel: +81-42-443-5980; E-mail: taki@pc.uec.ac.jp (M.T.)

^b *Department of Biological Systems Engineering, Graduate School of Biology-Oriented Science and Technology, KINDAI University, 930 Nishimitani, Kinokawa, Wakayama 649-6493, Japan.*

Tel: +81-736-77-3888; E-mail: miya@waka.kindai.ac.jp (N.M.)

^c *Department of Chemistry and Bioscience, Graduate School of Science and Engineering, Kagoshima University, 1-21-35 Korimoto, Kagoshima, Kagoshima 890-0065, Japan.*

[§] *Current affiliation: Tokyo Metropolitan Industrial Technology Research Institute, 2-4-10 Aomi, Koto-ku, Tokyo 135-0064, Japan.*

Supplemental figures

S2-S8

Materials and methods

S9-S23

Supplemental references

S23-24

Supplemental figures

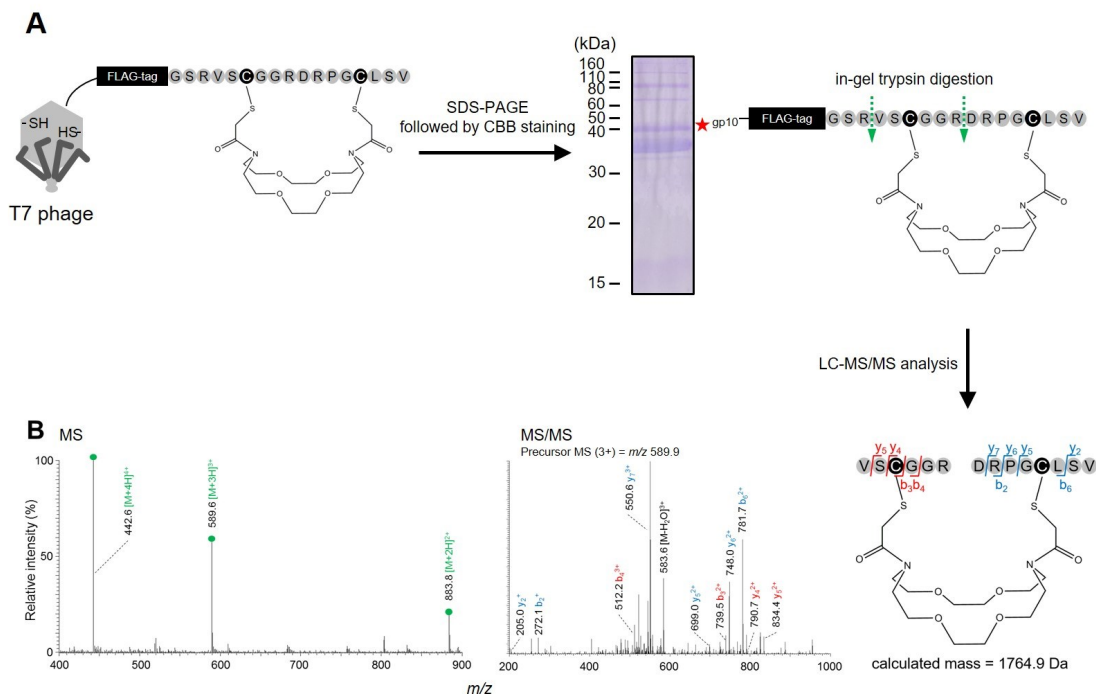


Figure S1. Tandem mass spectrometric analysis of the macrocyclic cryptand structure displayed on T7 phage. (A) A model T7 phage monoclonal, modified by the designed diazacrown precursor (*i.e.*, cr2 in Fig. 2) via the 10BASE_d-T, was separated into protein subunits by SDS-PAGE. After coomassie brilliant blue staining (upper middle panel), the protein band corresponding to the macrocycle-fused gp10 (pink asterisk) was excised and subjected to in-gel trypsin digestion followed by LC-MS/MS analysis. A green arrow indicates the trypsin cleavage sites. (B) MS spectrum (left panel). A series of multiple charged ions (green circles) were detected, and consistent with calculated m/z values of the cleaved macrocycle (lower right panel). From the parent ion of $m/z = 3$, we obtained an expected MS/MS spectrum (lower middle panel).

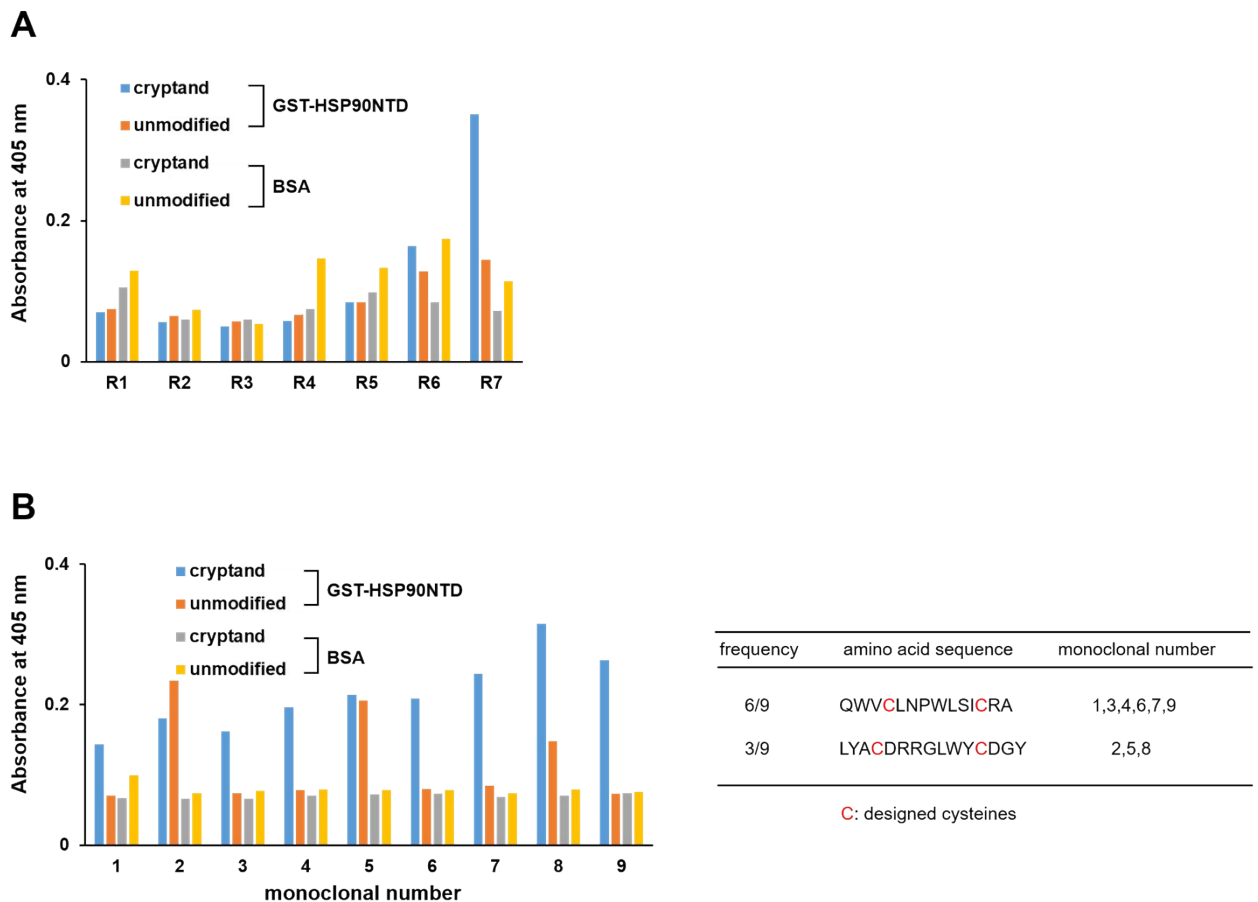


Figure S2. Biopanning against GST-Hsp90NTD using the library of cryptand-like structures (-SGGG-X₃-C*-X₇-C*-X₃; Cys were conjugated with the designed cr2 precursor: 1,10-diaza-18-crown-6 ether). (A) For the cryptand-modified bars (blue and gray), T7 phage polyclones after each round (R) of biopanning were modified with cr2. Both the modified and unmodified T7 phage polyclones were subjected to ELISA. GST-Hsp90NTD and bovine serum albumin (BSA) were used as the target and a mock (*i.e.*, target-unrelated) proteins, respectively. (B) Among 9 randomly chosen single T7 phage plaques after the 7 rounds of biopanning, 6 clones had positive signals for GST-Hsp90NTD binding only when cr2 ether was conjugated to the designated Cys on the displaying peptide.

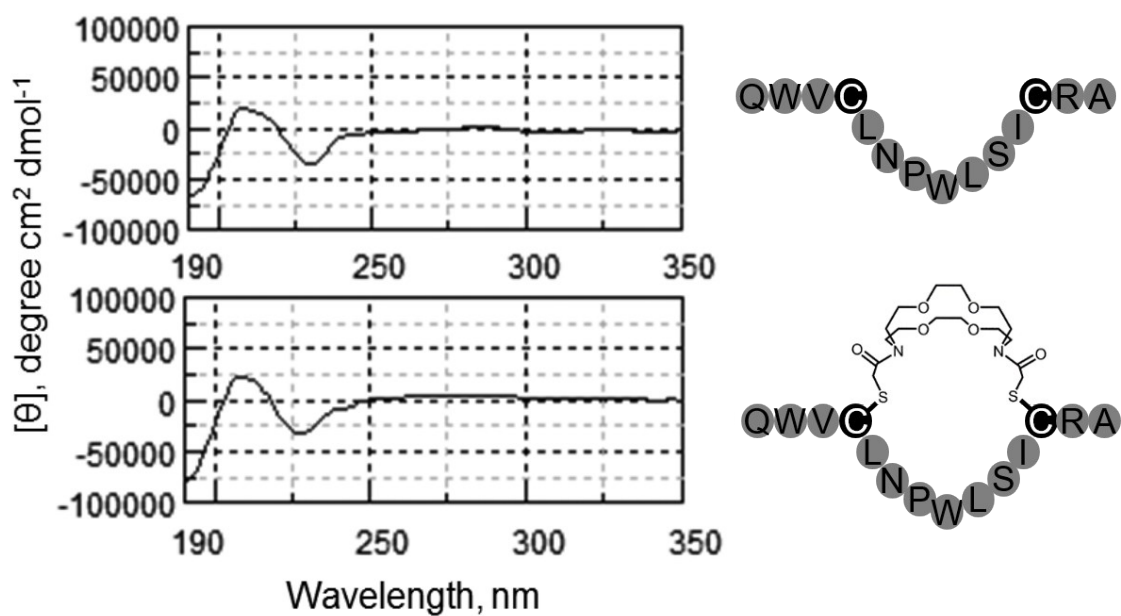


Figure S3. CD spectra of the selected peptide alone (upper) and the corresponding Hsp90NTD-binding cryptand (lower). The amino acid sequence of the selected peptide is $\text{H}_2\text{N-QWVCLNPWLSICRA-OH}$.

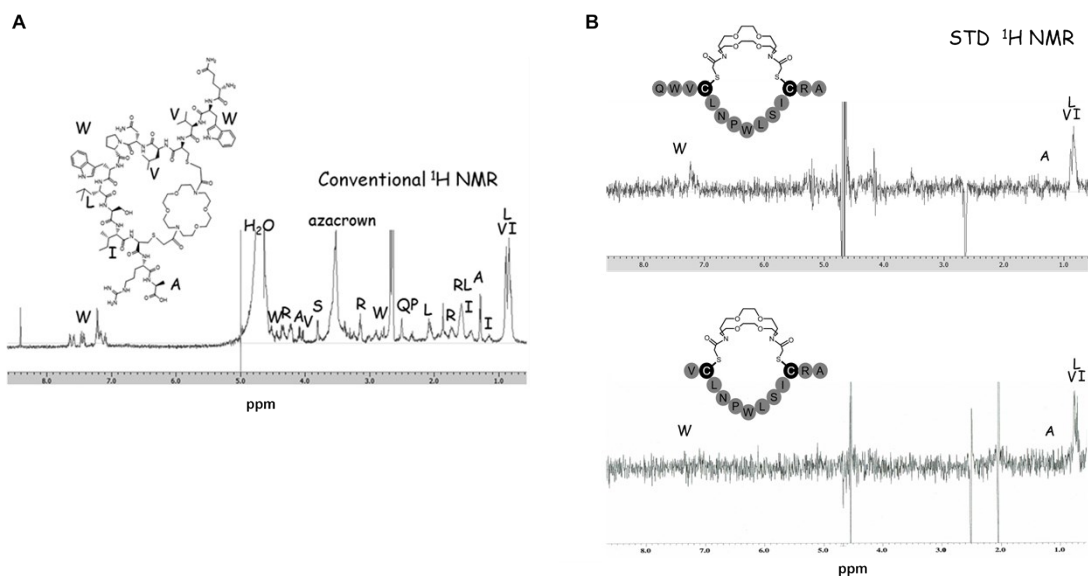


Figure S4. Identification and epitope mapping of the cryptand upon Hsp90NTD binding on the basis of saturation transfer difference-nuclear magnetic resonance (STD-NMR) measurement. (A) Conventional ^1H NMR spectrum of the cryptand. Each amino acid peak, shown in a single letter, was identified from a combination of different two-dimensional NMR measurements (*e.g.*, ^1H - ^1H COSY). Ratios of all integral curves (omitted) were identical to the theoretical values. (B) STD-NMR spectra of the full-length (upper) and QW-deleted (lower) cryptands at the same molar concentrations. Among the hydrophobic side chains of amino acids in the cryptand, tryptophan (W) at the N-terminal lariat and some of leucine (L), isoleucine (I), and valine (V) were important for the Hsp90 binding, whereas W in the middle of the bicyclic structure and alanine (A) were not.

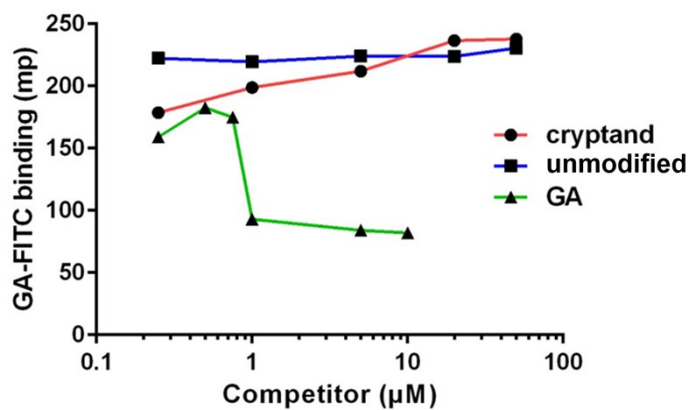


Figure S5. Competitive binding assay to confirm that the cryptand did not bind to the ATP-binding site of Hsp90NTD. Non-labeled geldanamycin (abbreviated as GA), which is known to bind to the site, and the unmodified selected peptide (*i.e.*, H₂N–QWVCLNPWLSICRA–OH) were served as a positive and a negative controls, respectively. The Hsp90NTD-binding cryptand did not compete with a fluorophore-conjugated GA (abbreviated as GA–FITC), or possibly might enhance binding of GA–FITC to Hsp90NTD.

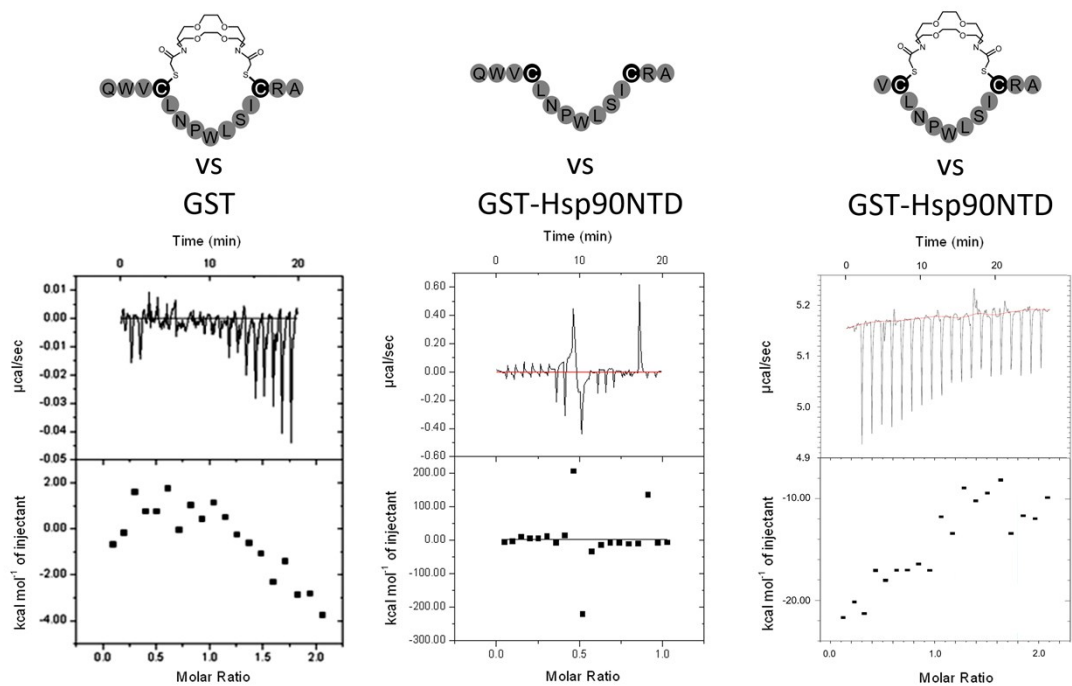


Figure S6. Isothermal titration calorimetry (ITC) profiles of titrations of GST with cryptand (left), GST-Hsp90NTD with the unmodified selected peptide (*i.e.*, H₂N–QWVCLNPWLSICRA–OH) (middle), and GST-Hsp90NTD with QW-deleted cryptand (right), respectively. The cryptand exclusively bound to Hsp90NTD (see Fig. 3C in the main text), not to GST. The azacrown moiety and N-terminal lariat were essential for the binding.

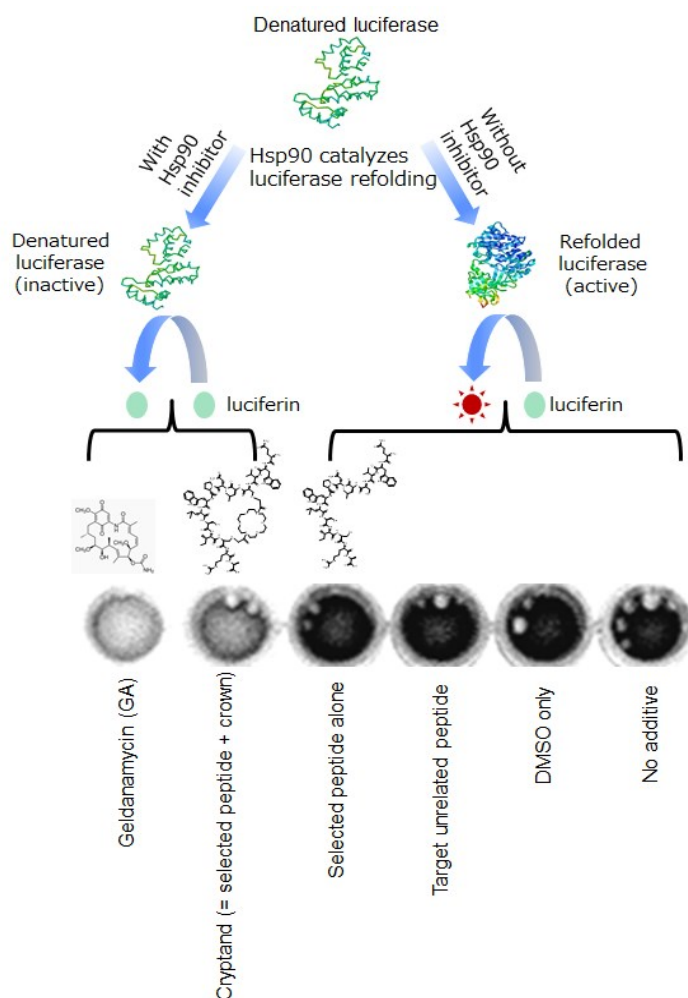
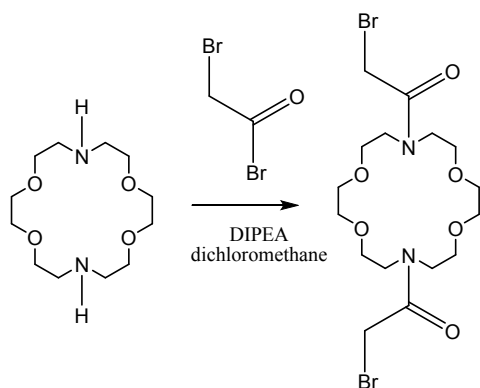


Figure S7. In vitro Hsp90 inhibition activity of the selected cryptand was estimated by densitometric analysis of luciferin luminescence using denatured luciferase / rabbit reticulocyte lysate (RRL) system.¹ The cryptand, made from the selected peptide and azacrown, blocked the refolding of thermally denatured firefly luciferase, which was supposed to be catalyzed by the Hsp90 chaperone machinery in RRL. In contrast, the selected peptide alone (without possessing the azacrown moiety) did not inhibit the Hsp90 activity, which supports the ITC result of the unmodified peptide (Fig. S6, middle). Geldanamycin, a well-known Hsp90 inhibitor, was served as a positive control. A target-unrelated peptide, whose amino acid sequence of is $\text{NH}_2\text{-DQLDRFYWS-OH}$, was served as a negative control. Each of the inhibitor candidate was once dissolved in dimethyl sulfoxide (DMSO) as a stock solution, and mixed with whole assay solution.

Materials and methods

Synthesis of 1,1'-(1,4,10,13-tetraoxa-7,16-diazacyclooctadecane-7,16-diyl)bis(2-bromoethanone)



1,1'-(1,4,10,13-tetraoxa-7,16-diazacyclooctadecane-7,16-diyl)bis(2-bromoethanone) (2Br-azacrown; **1**)² was prepared as previously reported³ with minor modifications. Briefly, 1,4,10,13-tetraoxa-7,16-diazacyclooctadecane (0.30 g, 1.1 mmol; cat. No. 295809, Sigma-Aldrich) and *N,N*-diisopropylethylamine (0.60 mL, 3.3 mmol) were mixed in 2.0 mL of dichloromethane solution on ice. Then, bromoacetyl bromide (0.30 mL, 3.3 mmol; cat. No. B56412, Sigma-Aldrich) was gradually added, and the mixture was stirred for 5.5 hours initially at 0 °C and then at room temperature. Then the solvent was evaporated. The crude reaction product was purified by reverse-phase middle pressure liquid chromatography (Yamazen ODS column 26 × 300 mm, flow rate 20 mL/min with gradient 5–100% MeOH in pure water over 40 min). The fractionated sample was lyophilized to afford brownish oil (0.15 g, 30% yield). LC-MS/absorbance chromatogram and ¹H NMR (500 MHz, CDCl₃) spectrum of the purified 2Br-azacrown are shown in below (Fig. S8).

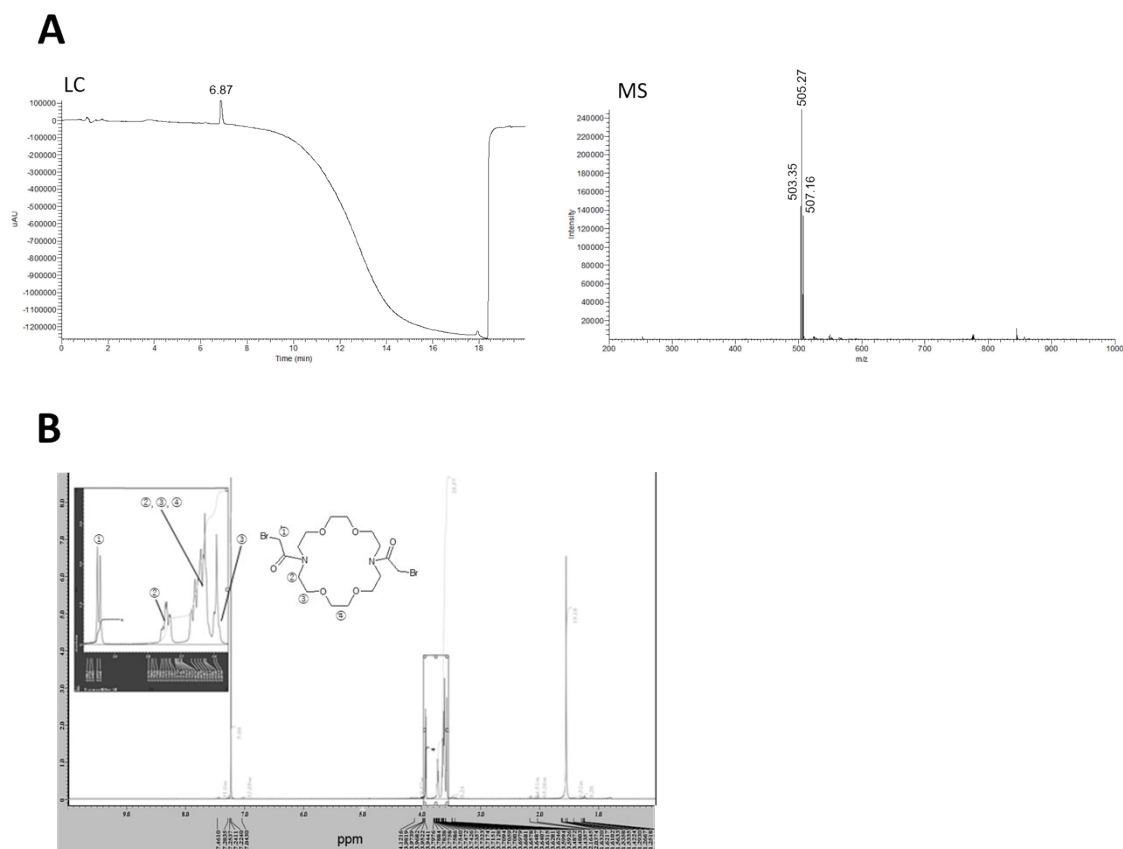


Figure S8. (A) LC-MS/absorbance chromatogram, and (B) ¹H NMR spectrum of 1,1'-(1,4,10,13-tetraoxa-7,16-diazacyclooctadecane-7,16-diyl)bis(2-bromoethanone). For the chromatogram, total absorbance of ultraviolet region was shown in the left panel. Observed *m/z* values from a parent ion of 6.87 minutes (*i.e.*, 503.35, 505.27, and 507.17 in the right panel) correspond to the theoretical *m/z* values of 503.0, 505.0 and 507.0, respectively; the intensity ratios of these three signals indicate that two bromide atoms were conjugated in a single molecule.

Construction of a library of cryptand-like structures via the 10BASE_d-T

Cyclization of a displaying peptide (or its library) on T7 phage via the gp10 based-thioetherification (10BASE_d-T) was performed as described previously.⁴ Standard reaction conditions are the following: T7 phage particles (approximately 1.0×10^{11} plaque forming units) were well suspended by sonication or vortex in 700 μ L of Dulbecco's phosphate buffered saline (D-PBS) supplemented with 400 mM NaCl. After centrifugation at 12,000 rpm for 5 minutes at room temperature, the supernatant was

mixed with neutralized tris(2-carboxyethyl)phosphine (TCEP) aqueous solution at a final concentration of 500 μ M at 4 °C: optimal molar concentration of 2Br-azacrown was estimated at 0.5 to 1.0 mM by a previous method.⁵ Aqueous solution of 2Br-azacrown was added at a final concentration of 500 μ M, and the mixture was incubated at 4 °C for 3 hours in the dark. To inactivate the unreacted 2Br-azacrown, 2-mercaptoethanol was added to the mixture at a final concentration of 5 mM, and further incubated at 4 °C for several minutes. The T7 phage particles were precipitated with a mixture of polyethylene glycol 6000 and sodium chloride to final concentrations of 5% w/v and 0.5 M, respectively. After centrifugation at 15,000 rpm for 10 minutes at 4 °C, the precipitate was dissolved in an appropriate buffer. We also examined the infectivity of the modified T7 phage library by plaque assay, and confirmed that the infectivity titers before and after the chemical modification did not show significant changes each other, like every case in our previous results.⁴⁻⁷

Preparation of GST-Hsp90NTD, GST-Hsp90MD, and GST-Hsp90CTD

N-terminal domain (NTD: residues of 9–236) of human Hsp90 α , was prepared as described previously with minor modifications.^{4, 8, 9} Briefly, pGEX-4T-3 vector encoding fragments of Hsp90 gene was introduced into *E. coli* BL21 (DE3) strain. The transformants were precultured overnight at 37 °C in 2 mL of LB medium supplemented with 100 μ g/mL ampicillin, and then transferred to a 150 mL of fresh LB medium. After incubation for 1 hour 35 minutes at 37 °C, isopropyl β -D-1-thiogalactopyranoside (IPTG) was added at a final concentration of 0.2 mM, and the cells were further cultured for overnight at 20 °C. The cells were harvested, and suspended in an ice-cold lysis buffer (50 mM Tris-HCl (pH 8), 300 mM NaCl, 1 mM EDTA, 5 mM 2-mercaptoethanol, 0.5 % w/v Triton X-100, and 1 \times cComplete protease inhibitor cocktail minus EDTA from Roche). After cell disruption by ultrasonication, the crude cell extract was centrifugated at 20,000 \times g for 10 min at 4 °C, followed by a 0.42 μ m membrane spin-filter. The supernatant was incubated with glutathione sepharose 4B beads (GE Healthcare) for overnight at 4 °C. After several washings with the lysis buffer, GST-Hsp90NTD on the beads was eluted with an elution buffer

containing phosphate buffered saline (PBS, pH 8 adjusted with NaOH/KOH), 1 mM DTT, and 43 mM reduced glutathione. GST-Hsp90NTD was enriched using an ultrafiltration column (Vivaspin 20 MWCO 10 kDa, GE Healthcare), and the buffer was changed to 20 mM phosphate (pH 7.5). GST-Hsp90 middle (MD: 272–617) and C-terminal domains (CTD: 629–732) were also expressed and purified in the same way.⁴

Biotinylation of GST-Hsp90NTD

GST-Hsp90NTD (56 g/L) in 20 mM phosphate buffer (pH 7.5) was mixed with biotinamidohexanoic acid 3-sulfo-N-hydroxysuccinimide ester sodium salt (Sigma, MO, USA) at a final concentration of 2.2 mM, and incubated at 4 °C overnight. For desalination, Zeba™ Spin Desalting Columns (Thermo Fisher Scientific, MA, USA) was used with centrifugation at 3,000 rpm for 4 minutes at 4 °C. The degree of biotinylation of GST-Hsp90NTD was quantified by a densitometric analysis from Western blotting reported previously;⁴ it was estimated that approximately 1.4 molecules of biotin were conjugated to a single GST-Hsp90NTD molecule (data not shown).

Biopanning

Biopanning was performed as described previously⁴ with minor modifications. Biotinylated-GST-Hsp90NTD (300 pmol) was immobilized on streptavidin-coupled magnetic beads. For biopanning, approximately 1.0×10^{11} pfu of a T7Select10 library (-SGGG-X₃-C-X₇-C-X₃; X represents any randomized amino acid) was modified with 2Br-azacrown via the 10BASE₄-T. After the cyclization, the T7 phage library was dissolved in a selection buffer (D-PBS supplemented with 1% v/v TritonX-100 and 1% w/v BSA). To remove non-specific binders (*i.e.*, beads, streptavidin, and GST binders), the modified T7 phage library was pre-incubated with streptavidin-coupled magnetic beads and GST-immobilized ones for 3 hours at 4 °C, respectively. The supernatant was further incubated with the GST-Hsp90NTD-immobilized beads for 23 hours. The latter beads were washed three times with 200 μL of the selection buffer. Whole binding and washing processes were performed using an automated machine (Target Angler 8,

Tamagawa Seiki, Japan). GST-Hsp90-bound phage was directly infected and amplified with *E. coli* BLT5403 strain. Stringent conditions were applied stepwise to each round by shortening the binding time and by increasing the washing frequency. After 7 rounds of biopanning, randomly chosen T7 phage monoclones were subjected to ELISA followed by DNA sequencing to identify the selected peptide.

Enzyme-linked immunosorbent assay (ELISA)

ELISA was performed as described previously⁴ with minor modifications. Each well of a 96-well plate (Maxisorp, Clear Flat Bottom Immuno Nonsterile 96-Well Plates, Thermo Scientific) was coated with 0.2 μ M GST-Hsp90NTD in D-PBS at 4 °C overnight. After discarding the solution in each well, TBS supplemented with 0.05% (v/v) Tween 20 and 0.5% (w/v) BSA was applied to the well and incubated for 1 hour at 18 °C with shaking using a maximizer (MBR 022UP, TAITEC, Japan). After washing with D-PBS supplemented with TritonX-100, approximately 1.0×10^{11} pfu of T7 phage in TBS supplemented with 0.5% (v/v) TritonX-100 was applied to the well and incubated for 1 hour at 18 °C with shaking using the maximizer. The plate was washed three times with TBS supplemented with 0.5 % (v/v) Triton X-100, and then GST-Hsp90NTD bound phage was incubated with T7 tail fiber monoclonal antibody (1:5,000 dilution, Merck Millipore, Germany) and anti-mouse IgG horseradish peroxidase linked antibody (1:5,000 dilution, Cell Signaling Technology, MA, USA). After washing with TBS supplemented with 0.5% (v/v) Triton X-100, a substrate solution (0.05 M citric acid, 0.02 M hydrogen peroxide, 0.4 mM 2,2'-azino-bis(3-ethylbenzothiazoline-6-sulfonic acid) diammonium salt, pH 4) was added, and the absorbance was quantified using a microplate reader equipped with a 405 nm band-pass filter (Bio-Rad, CA, USA).

Synthesis of Hsp90NTD-binding cryptand

The selected linear peptide (H₂N–QWVCLNPWLSICRA–OH) was chemically synthesized and characterized by GenScript Inc. (NJ, USA). For cyclization between the peptide and 2Br–azacrown **1** to afford the Hsp90NTD-binding cryptand, the peptide (10 mg, 5.9 μ mol) was dissolved in 54 mL of phosphate buffer (8 mM phosphate-Na, pH

7.4) at a final concentration of 0.10 mM, and then **1** (12.4 mg, 0.46 mM) and neutralized TCEP (0.50 mM) dissolved in trace amount of water were added. The mixture at a high-dilution condition was incubated for 3 hours at room temperature in the dark with shaking. To quench remaining 2Br-azacrown **1**, neat 2-mercaptoethanol (3.8 μ L, 1.0 mM) was further added to the reaction mixture. It was incubated for additional 5 minutes at room temperature in the dark with shaking, and then lyophilized. The lyophilizate was dissolved in 0.1% formic acid / 30% DMSO aqueous solution, and the cryptand was purified with a reverse-phase HPLC (Shimadzu, Japan) equipped with a XTerra Prep MS C18 column (10 \times 50 mm, Waters). The cryptand was separated using a 0–100% linear gradient of methanol containing 0.1% formic acid during 10 min at a flow rate of 4 mL per minute. The obtained cryptand (4.2 mg, 35% yield) was lyophilized and characterized by LC-MS/MS (liquid chromatography-mass spectrometry/mass spectrometry) (see below; Fig. S9).

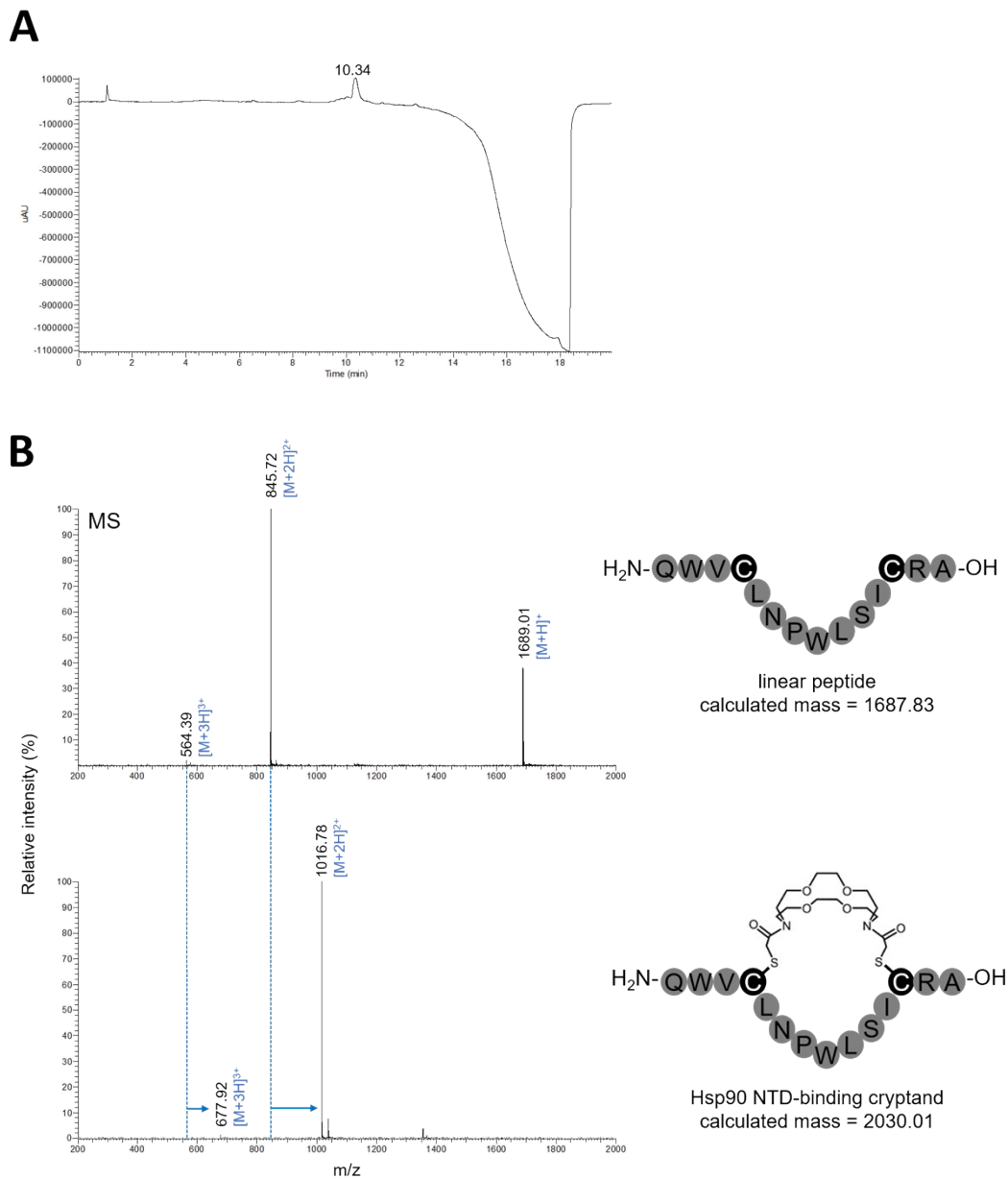


Figure S9. Identification of the Hsp90NTD-binding cryptand: LC/absorbance chromatogram (A), and corresponding MS chart (B, lower) at the retention time of 10.34 min. MS chart of the selected linear peptide before cyclization was also shown (B, upper). For the chromatogram, total absorbance of ultraviolet region was shown. Although most of the b and y MS/MS fragments of the linear peptide (H₂N–QWVCLNPWLSICRA–OH) could be identified before the cyclization (data not shown), only a limited numbers of MS/MS fragments could be seen after the cyclization.

Synthesis of QW-deleted cryptand

The QW-deleted linear peptide (H₂N–VCLNPWLSICRA–OH) was chemically synthesized and characterized by GenScript Inc. (NJ, USA). For cyclization between the peptide and 2Br–azacrown **1** to afford the QW-deleted cryptand, the peptide (5.2 mg, 3.8 μmol) was dissolved in 35 mL of phosphate buffer (8 mM phosphate-Na, pH 7.4) at a final concentration of 0.1 mM, and then **1** (8.0 mg, 0.46 mM) and neutralized TCEP (0.50 mM) dissolved in trace amount of water were added. The mixture at a high-dilution condition was incubated for 3 hours at room temperature in the dark with shaking. To quench remaining 2Br–azacrown **1**, neat 2-mercaptoethanol (2.5 μL, 1.0 mM) was further added to the reaction mixture. It was incubated for additional 20 minutes at room temperature in the dark with shaking, and then lyophilized. The lyophilizate was dissolved in 0.1% formic acid / 30% DMSO aqueous solution, and the cryptand was purified with a reverse-phase HPLC (Shimadzu, Japan) equipped with a XTerra Prep MS C18 column (10 × 50 mm, Waters). The QW-deleted cryptand was separated using a 0–100% linear gradient of methanol containing 0.1% formic acid during 10 min at a flow rate of 4 mL per minute. The obtained QW-deleted cryptand (0.3 mg, 4.6% yield) was lyophilized and characterized by LC-MS/MS (see below; Fig. S10).

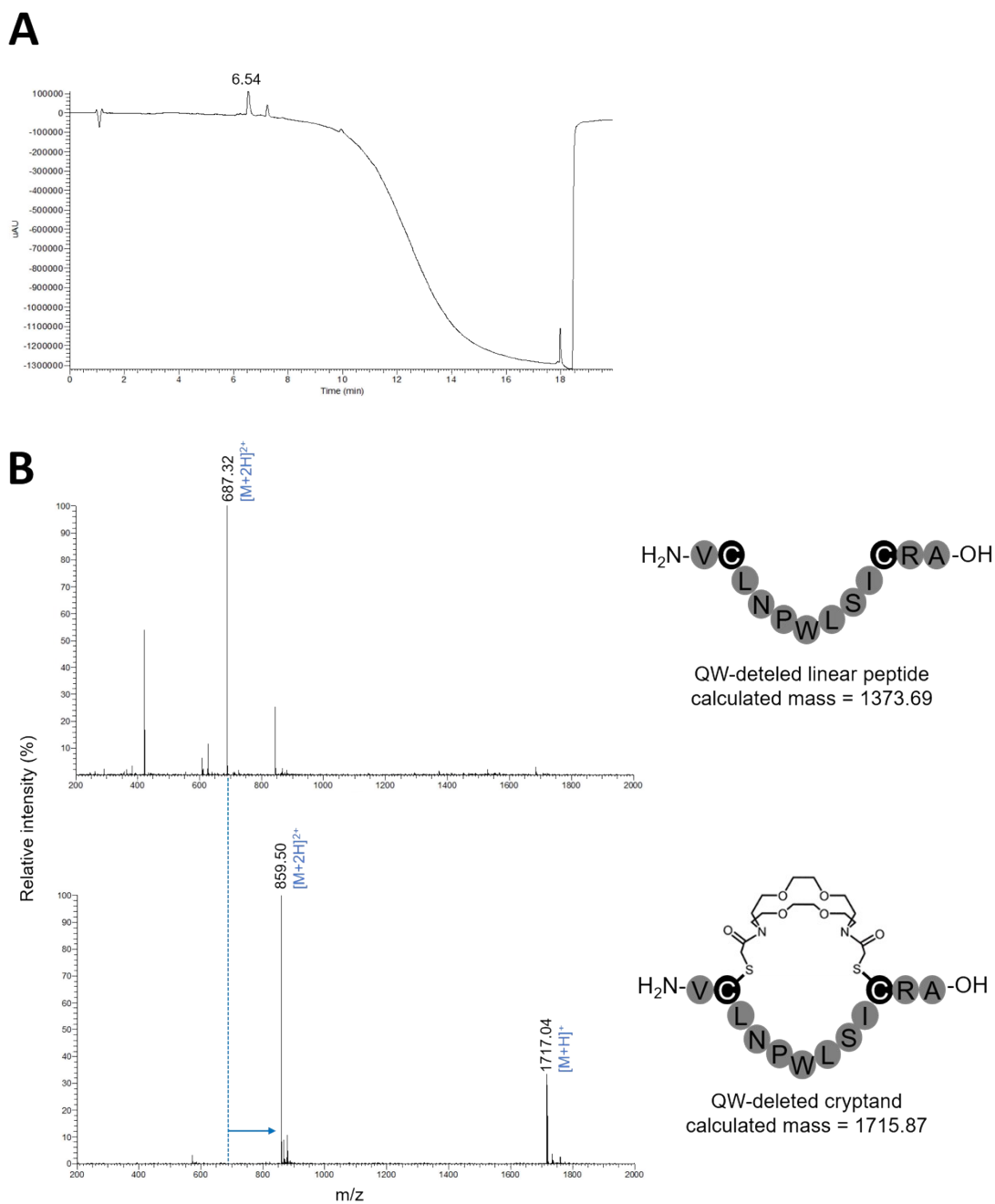


Figure S10. Identification of the QW-deleted cryptand: LC/absorbance chromatogram (A), and corresponding MS chart (B, lower) at the retention time of 6.54 min. MS chart of the QW-deleted linear peptide before cyclization was also shown (B, upper). For the chromatogram, total absorbance of ultraviolet region was shown. Only a limited numbers of MS/MS fragments could be seen after the cyclization.

CD spectra of Hsp90NTD-binding cryptand

Circular dichroism (CD) spectra were recorded for both selected linear peptide and cryptand, as reported previously.⁴ Briefly, the compounds were dissolved in phosphate buffer (20 mM phosphate, pH 7.4) at a final concentration of 20 μ M, and the spectra were recorded on a CD spectrometer (J-720W, JASCO, Japan) at 25 °C using a 1 cm path-length quartz cell (Figure S3). In either of them, typical peaks representative of tertiary structures of β -turn¹⁰ were observed.

Isothermal titration calorimetry (ITC)

ITC experiment was performed using MicroCal iTC₂₀₀ (GE Healthcare). GST-tagged Hsp90NTD was enriched using an ultrafiltration column (Vivaspin column 500 MWCO 10 kDa, GE Healthcare), and the buffer was changed to phosphate buffer (20 mM phosphate-KOH, pH 7.2, 50 mM NaCl, 1 mM TCEP). Protein concentration was determined by Bradford assay, and double-checked by molar absorption coefficient at 280 nm. For titration experiment, protein (*e.g.*, GST-Hsp90NTD or GST) and ligand (*e.g.*, cryptand, linear peptide, or QW-deleted cryptand) were diluted into 5 μ M and 50 μ M, respectively. Titrations were performed at 25 °C. Injection parameters were the following: 2 μ L volume, 4 sec duration, 60 sec spacing, and 5 sec filter period. Reference power was set to 5 μ cal/s. Data were analyzed with Origin software 7.0 (MicroCal). Curve fitting was performed using 1:1 interaction model.

Hsp90 inhibition assay using denatured luciferase

In vitro Hsp90 inhibition activity of the selected cryptand was estimated on the basis of densitometric analysis for measuring Hsp90-dependent refolding of thermally denatured luciferase, according to a reported method¹ with a slight modification. Briefly, 15 μ L of rabbit reticulocyte lysate (RRL, Promega) supernatant was mixed with 125 μ L of a refolding buffer. Final concentration of the refolding buffer is: 80 mM Tris-HCl (pH 7.7), 8 mM Mg(OAc)₂, 0.30 M KCl, 12 mM ATP, 4 mM *DL*-dithiothreitol (DTT), 20 mM creatine phosphate, and 0.8 mg/mL creatine phosphokinase. The solution was divided into 30 μ L, mixed with 1 μ L (0.75 nmol; final 25 μ M) of each Hsp90 inhibitor

candidate stock solution (0.75 mM in dimethyl sulfoxide (DMSO)), and incubate at room temperature with gentle shaking. Then, 3.2 pmol of thermally denatured luciferase (at 40 °C, 10 min.) in a buffer of 25 mM Tricine–HCl (pH 7.8), 8 mM MgSO₄, 0.1 mM ethylenediaminetetraacetic acid (EDTA), 10 mg/mL BSA, 10% glycerol, and 1% Triton X-100, was mixed into each sample, and the mixture was incubated at room temperature for 30 minutes to promote the refolding of the denatured luciferase by native Hsp90 in RRL. Then, it was mixed with 30 µL of an assay buffer. Final concentration of the assay buffer is: 75 mM Tricine-HCl (pH 7.8), 24 mM MgSO₄, 300 µM EDTA, 2 mM DTT, 313 µM *D*-luciferin, 640 µM coenzyme A, 660 µM ATP, 150 mM KCl, 10% (v/v) Triton X-100, 20% (v/v) glycerol, and 3.5% DMSO. An estimated final concentration of Hsp90 was 140 nM.¹¹ Luminescence from the mixture on 96-well plate was analyzed by a conventional imager (Gel Doc XRS+; Bio-Rad, Hercules, CA, USA).

Fluorescence polarization (FP) assay

Fluorescence polarization was measured using HYBRID-3000ES system (Photoscience, Tokyo, Japan) equipped with appropriate filters (Ex. 480 nm and Em. 535 nm). The instrument was operated in a static mode. For competition assays, various concentrations of compounds were pre-incubated with GST-Hsp90NTD (110 pmol, 550 nM) in D-PBS supplemented with 1 mM TCEP for 10 min at room temperature. After addition of fluorophore-conjugated GA (abbreviated as GA–FITC; 4 pmol, 20 nM), the mixture was incubated for 5 min at 30 °C, and then fluorescence polarization was measured. GA–FITC and non-labeled geldanamycin were purchased from Enzo Life Sciences (cat No. BML-EI361-0001, Farmingdale, NY, USA) and StressMarq (cat No. SIH-111A/B, Victoria, BC, Canada), respectively.

Nucleic magnetic resonance (NMR) measurements

NMR experiments including two-dimensional measurements and saturation transfer difference (STD) ones were performed at 30 °C by using a 500 MHz spectrometer (JNM-ECA500, Jeol Resonance, Japan) according to a reported procedure.⁷ Briefly, proton assignments of cryptand were performed by using a conventional set of 2D

spectra: 2D ^1H - ^1H COSY, totally correlated spectroscopy (TOCSY) with 150 ms mixing time, nuclear Overhauser effect correlated spectroscopy (NOESY) with 0.5 s mixing time. Cryptand (0.32 mM) was dissolved in 10 mM phosphate (pH 7.4) / D_2O with 10% $\text{DMSO-}d_6$. For the STD measurements, a selective saturation of GST-Hsp90NTD with a saturation time of 4.0 s was achieved by a train of Gauss-shaped pulses of 60 ms. On-resonance and off-resonance irradiations of GST-Hsp90NTD were performed at a chemical shift of 0.5 and -10 ppm, respectively. The STD spectra were taken by subtraction of the on- and off-resonance spectrum.

Photo-crosslinking between SDA-conjugated cryptand and GST-Hsp90NTD

Succinimidyl-ester diazirine (SDA, Thermo Scientific™, MA, USA; 0.9 mM) and cryptand (0.23 mM) were dissolved in 11 μL of D-PBS with 9% DMSO. After incubation for 4.5 hours at 4 °C, 0.1 μL of 2 M Tris-HCl (pH 8; final 18 mM) was added to the mixture, and further incubated at 4 °C for 15 minutes to quench remaining SDA. The mixture was diluted to 40 μL with D-PBS, and then GST-Hsp90NTD (9 μM) was dissolved in the mixture. After incubation for 30 minutes at 4 °C, photo-crosslinking of GST-Hsp90NTD with the SDA-conjugated cryptand was carried out with an irradiation of a 365 nm light by using a handheld UV lamp (6 W, UVGL-58, 100 V; Funakoshi, Japan) for 1 hour at room temperature. It was separated by 10% SDS-PAGE using a large gel, and a band around 55 kDa was excised from the gel (Fig. S11). The protein in the gel was reduced with 25 mM DTT at 65 °C for 10 min, and then alkylated with 55 mM iodoacetamide at room temperature for 60 min in the dark. Digestion was carried out with modified trypsin (Promega, Madison, WI, USA) at 37 °C overnight. The digested peptide fragments were spotted on a stainless plate with α -cyano-4-hydroxycinnamic acid as a matrix, and analyzed by matrix assisted laser desorption/ionization–time-of-flight (MALDI-TOF) MS using an UltrafleXtreme (Bruker Daltonics, Billerica, MA, USA) instrument.

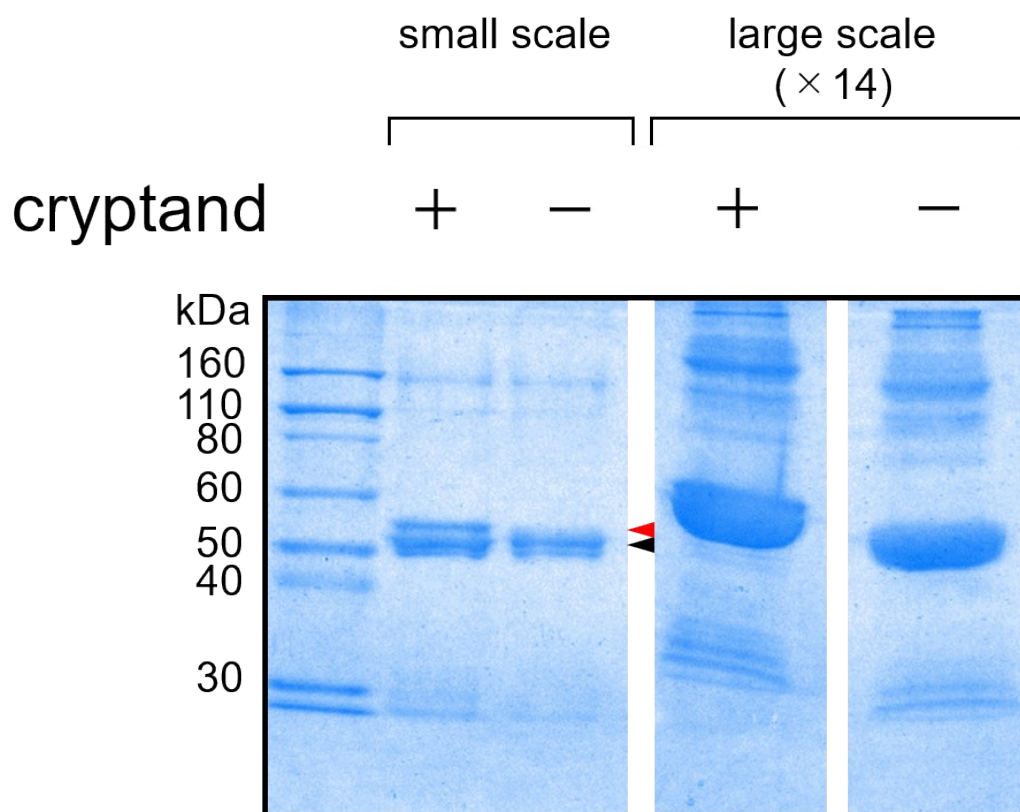


Figure S11. Site-specific conjugation between GST-Hsp90NTD and SDA-conjugated cryptand, confirmed by 10% SDS-PAGE. Plus (+) and minus (-) stand for presence and absence of the GST-Hsp90NTD-binding cryptand, respectively. The cryptand-conjugated GST-Hsp90NTD (red arrow) and unreacted GST-Hsp90NTD (black arrow) were visualized by CBB staining. The bands around 55 kDa in the large-scale sample were excised and subjected to in-gel trypsinization followed by MALDI-TOF-MS analysis.

Molecular dynamics (MD) simulations and docking simulations

To design a core structure of the artificial macrocycle, 2-microseconds MD simulations for each core candidate (cr1, cr2, cr3, cr4, and cr5 in Fig. 2, respectively) were performed using Generalized AMBER Force Field (GAFF).¹² The simulations were carried out in the isothermal-isobaric (NPT) ensemble (300K and 1 bar) with SPCE water molecules and 150 mM of Na⁺ and Cl⁻ ions using GROMACS 5.1 software. Distributions of the distance between N-N and average tunneling ratios of the dihedral angles in the core candidates were used as evaluating the fluctuation. The average

tunneling ratios of dihedrals in Fig. 2C were derived from the number of the rotation of the dihedral angle around nitrogen atoms (Fig. 2B) in the simulations. For the cyclic cryptand precursors, the geometric fluctuation of the smallest core compound (*i.e.*, cr1) was the smallest, and all of the candidates (*i.e.*, cr1, cr2, and cr4) have two peaks in the distance between nitrogen-nitrogen atoms (N-N). The fluctuations of the non-cyclic precursors (*i.e.*, cr3 and cr5) were too large. From all of the above simulation results, we chose cr2 as the best precursor because it possessed both **medium-firmness** and geometric homogeneity.

The MD simulations of the crown-like binder, the cryptand-like binder, and Hsp90NTD were performed using a modified AMBER14sb Force field in which a force field of middle molecules was mixed altogether with the standard parameters for high-molecular weight. Each simulation time was 2-microseconds in the NPT ensemble with the same conditions as the MD simulations of the core candidates. Figure S12 shows the most favorable structure of each simulation. The distribution of the distance between N-N in the cryptand-like binder or crown-like binder suggests that the cryptand-like binder was more rigid than the crown-like binder (Fig. 2E).

In the MD simulation of the cryptand-like binder, the interaction between Trp₂ and Arg₁₃ was frequently observed (Fig. S12D), which seems to stabilize the structure of the cryptand-like binder. Furthermore, the STD-NMR experiment explained that at least one Trp in the cryptand-like binder dominantly interacted with Hsp90NTD (Fig. S4B, upper), and the ITC profile of the QW-delated cryptand (Fig. S6, right) suggested that Gln₁ and Trp₂ are necessary for the cryptand-like binder to keep the high affinity. Thus, Trp₂ can be the critical residue for the binding to Hsp90NTD.

The computational docking simulations for the favorable structures between Hsp90NTD and the cryptand-like binder were carried out by AutoDock Vina.¹³ A docking region possessing a cubic grid involved the whole Hsp90NTD. In usual cases, it is difficult to perform a flexible docking using a large ligand (*e.g.*, the cryptand-like binder) in AutoDock Vina, because it is hard to prepare all possible conformations. Nevertheless, we performed a combination of flexible docking and induced fit, because we assume that the conformation of the cryptand-like binder would not be changed

drastically before/after docking due to the rigidity. The results of the docking simulations suggest that the cryptand-like binder bound to the β -sheet regions in Hsp90NTD (Fig. 4).

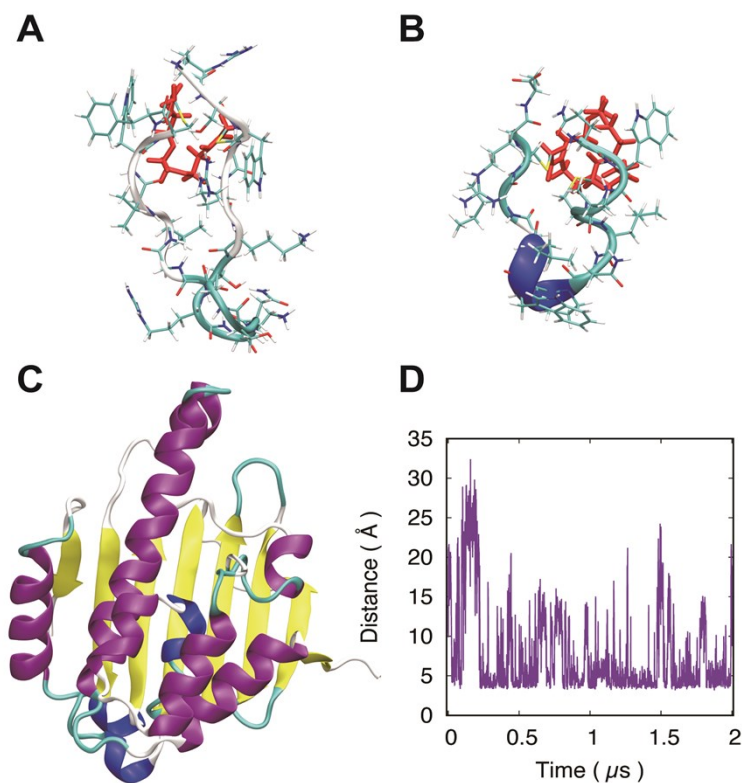


Figure S12. The most favorable structures of (A) crown-like binder, (B) cryptand-like binder, and (C) Hsp90NTD. The crown and cryptand precursors (*i.e.*, cr3 and cr2, respectively) were highlighted in red. Helices and β -sheets were shown in purple and yellow, respectively. (D) Time dependency of a distance between Trp₂ and Arg₁₃ in the cryptand-like binder during a long-time MD simulation.

Supplemental references:

1. J. Davenport, M. Balch, L. Galam, A. Girgis, J. Hall, B. S. Blagg and R. L. Matts, *Biology (Basel)*, 2014, **3**, 101-138.
2. R. Y. Yang, C. Y. Bao, Q. N. Lin and L. Y. Zhu, *Chinese Chemical Letters*, 2015, **26**, 851-856.

3. M. Pietraszkiewicz, R. Gasiorowski, Z. Brzozka and W. Wroblewski, *Journal of Inclusion Phenomena and Molecular Recognition in Chemistry*, 1993, **14**, 237-245.
4. K. Fukunaga, T. Hatanaka, Y. Ito, M. Minami and M. Taki, *Chem Commun (Camb)*, 2014, **50**, 3921-3923.
5. Y. Tokunaga, Y. Azetsu, K. Fukunaga, T. Hatanaka, Y. Ito and M. Taki, *Molecules*, 2014, **19**, 2481-2496.
6. K. Fukunaga, T. Hatanaka, Y. Ito and M. Taki, *Molecular Biosystems*, 2013, **9**, 2988-2991.
7. M. Taki, H. Inoue, K. Mochizuki, J. Yang and Y. Ito, *Analytical Chemistry*, 2016, **88**, 1096-1099.
8. M. Minami, M. Nakamura, Y. Emori and Y. Minami, *European Journal of Biochemistry*, 2001, **268**, 2520-2524.
9. S. Murata, Y. Minami, M. Minami, T. Chiba and K. Tanaka, *Embo Reports*, 2001, **2**, 1133-1138.
10. S. M. Kelly and N. C. Price, *Current Protein & Peptide Science*, 2000, **1**, 349-384.
11. V. Daniel, A. B. Maksymowych, E. S. Alnemri and G. Litwack, *J Biol Chem*, 1991, **266**, 1320-1325.
12. **J. Wang**, R. M. Wolf, J. W. Caldwell, P. A. Kollman and D. A. Case, *Journal of Computational Chemistry*, 2004, **25**, 1157-1174.
13. O. Trott and A. J. Olson, *Journal of Computational Chemistry*, 2010, **31**, 455-461.